L70 Life Prediction for Solid State Lighting Using Kalman Filter and Extended Kalman Filter Based Models

Pradeep Lall[(1)], Junchao Wei[(1)], Lynn Davis[(2)]
[(1)] Auburn University
Department of Mechanical Engineering
NSF-CAVE3 Electronics Research Center
Auburn, AL 36849
[(2)] RTI International, Research Triangle Park, NC 27709
Tele: (334) 844-3424
E-mail: lall@auburn.edu

Abstract

Solid-state lighting (SSL) luminaires containing light emitting diodes (LEDs) have the potential of seeing excessive temperatures when being transported across country or being stored in non-climate controlled warehouses. They are also being used in outdoor applications in desert environments that see little or no humidity but will experience extremely high temperatures during the day. This makes it important to increase our understanding of what effects high temperature exposure for a prolonged period of time will have on the usability and survivability of these devices. Traditional light sources "burn out" at end-of-life. For an incandescent bulb, the lamp life is defined by B50 life. However, the LEDs have no filament to "burn". The LEDs continually degrade and the light output decreases eventually below useful levels causing failure. Presently, the TM-21 test standard is used to predict the L70 life of LEDs from LM-80 test data. Several failure mechanisms may be active in a LED at a single time causing lumen depreciation. The underlying TM-21 Model may not capture the failure physics in presence of multiple failure mechanisms. Correlation of lumen maintenance with underlying physics of degradation at system-level is needed. In this paper, Kalman Filter (KF) and Extended Kalman Filters (EKF) have been used to develop a 70-percent Lumen Maintenance Life Prediction Model for LEDs used in SSL luminaires. Ten-thousand hour LM-80 test data for various LEDs have been used for model development. System state at each future time has been computed based on the state space at preceding time step, system dynamics matrix, control vector, control matrix, measurement matrix, measured vector, process noise and measurement noise. The future state of the lumen depreciation has been estimated based on a second order Kalman Filter model and a Bayesian Framework. The measured state variable has been related to the underlying damage using physics-based models. Life prediction of L70 life for the LEDs used in SSL luminaires from KF and EKF based models have been compared with the TM-21 model predictions and experimental data.

Introduction

The field of electric lighting is undergoing major revolution. We are in the process of transition to solid state lighting from the incandescent lighting that we have so grown used to and fond off. The LEDs (Light Emitting Diodes) have been used in a variety of applications including automotive headlights, residential lighting, industrial lighting, televisions and displays. Early indications are that LEDs will dominate the lighting market because of the LEDs' advantages compared to the traditional fluorescent light in the light efficiency, energy saving, improved physical robustness and long operating hours. Energy is one of the major grand challenges facing us in the 21st century. Lighting accounts for 17% of the worldwide electricity consumption. Non-OECD countries presently account for 82% of the increase in global energy usage. One possible way to address the growing demand for energy is to reduce the energy consumption on lighting [Baribeau 2012]. The U.S. Department of Energy has made a long term commitment to advance the efficiency, understanding and development of solid-state lighting (SSL) and is making a strong push for the acceptance and use of SSL products to reduce overall energy consumption attributable to lighting.

The transition to solid state lighting poses certain challenges. The industrial utilization of LEDs in extreme environments requires the LEDs have a good survivability under exposure to wide temperature excursions, humidity, and vibration. Consistency and reliability of SSL needs to be improved beyond the present generation. Challenging applications include: Automotive, Healthcare, and Horticulture. SSL luminaires are complex systems consisting of LEDs, Optics, Drive electronics, and Controls. Consumer electronics applications expected to function for only 1-3 years. Currently, it is not possible to qualify SSL luminaire lifetime of 10-years and beyond often necessary of high reliability applications, primarily because of lack of accelerated test techniques and comprehensive life prediction models. SSL devices comprises of several length scales with different failure modes at each level. There may be interactions between optics, drive electronics, controls and thermal design impact reliability. Accelerated testing for one sub-system may be too harsh for another sub-system. New methods are needed for predicting SSL reliability for new and unknown failure modes. Presently, there is scarcity of life distributions for LEDs and SSLs devices which are needed to assess the promised lifetimes.

LED failure is often addressed by the L70 lifetime, which is the time required for the LED lumen output to drop to 70- percent of the initial output or stated conversely, it indicates 70-percent lumen maintenance time. L70 life is presently

computed based on a minimum 6000 hours of LED testing using the LM-80 test method and TM-21 extrapolations of the LM-80 data. The TM-21 model relies on an exponential model of LED degradation for assessment of the L70 life. The underlying TM-21 model may not capture the failure physics in presence of multiple failure mechanisms. Since multiple failure mechanisms may be active in an LED or an SSL, the determination of single activation energy accurately may be challenging if not impossible. Further, the weighted average activation energy is based on large population statistics for a particular LED or SSL design and may or may not be applicable for the part of interest. In this paper, a new methodology for the L70 life prediction of LEDs has been developed based on the use of underlying physics based damage propagation models in conjunction with the Kalman Filter. Kalman filtering is a recursive algorithm that estimates the true state of a system based on noisy measurements [Kalman 1960, Zarchan 2000]. Previously, the Kalman Filter has been used for navigation [Bar-Shalom 2001], economic forecasting [Solomou 1998], and online system identification [Banyasz 1992]. Typical navigation examples include tracking [Herring 1974], ground navigation [Bevly 2007], altitude and heading reference [Hayward 1997], auto pilots [Gueler 1989], dynamic positioning [Balchen 1980], GPS/INS/IMU guidance [Kim 2003]. Application domains include GPS, missiles, satellites, aircraft, air traffic control, and ships. The ability of a Kalman filter to smooth noisy data measurements is utilized in gyros, accelerometers, radars, and odometers. Prognostication of failure using Kalman filtering has been demonstrated in steel bands and aircraft power generators [Batzel 2009, Swanson 2000, 2001]. Numerous applications in prognostics also exist for algorithms using more advanced filtering algorithms, known as particle filters. The state of charge of a battery was estimated and remaining useful life was predicted in [Saha 2009[a,b]].

Kalman Filter and Extended Kalman Filter Models have been used to estimate the future lumen state of the LED system, track the Lumen Maintenance degradation lines, and estimate the L70 life for the specific part of interest and determine remaining useful life. System state has been described in state space form using the measurement of the feature vector, velocity of feature vector change and the acceleration of the feature vector change. This model can be used to calculate acceleration factors, evaluate failure- probability and identify ALT methodologies for reducing test time. It is anticipated that the presented method could be used for health monitoring of large deployments of LEDs and SSL devices whether in street lighting or automotive applications and allow continual insight into the anticipated downtime for repair and replacement. Kalman Filter is used for linear- system tracking while the Extended Kalman Filter can be used for case in the non-linear system. Both algorithms can generate dynamic and updating estimations at each data points of interest, and then we can get the distribution of pseudo L70 life from those estimations. Model predictions have been compared with TM21 calculator. Degradation models used to capture the underlying physics of the LED and SSL system have been discussed. The cumulative failure distribution has been obtained, and the expected reliability computed with 95% confidence bounds.

Test-Vehicle and Experimental Data

In this paper, 10,000 hour test data acquired by Philips on the LUXEON Rebel LED has been used for model development. The dataset is titled DR05-1-LM80 [Philips 2012]. Data was acquired in accordance with the IES LM-80 standards, and the correlated color temperature (CCT) of the testing units is 3000K. Data at ambient air temperature of 55°C, 85°C, 105°C, and 120°C with LED currents in the range of 0.35A to 1A have been used for model development. Table 1 shows the scope of the input data set used for model development. A representative sample of the test product, commercially known as LUXEON LXM3-PW series LED, is shown in Figure 1. The surface temperature measurement location is shown in Figure 1. The surface temperature is lower than the ambient temperature by approximately 2°C in most cases. Each test condition has 25 samples. Lumen maintenance data has been reported along with the u' and v' measurements versus accelerated test time up to 10,000 hours of test time.

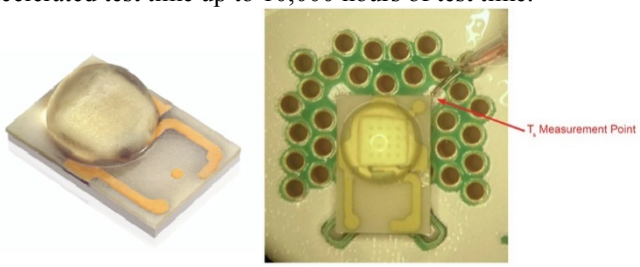

Figure 1: LED Test Product [Philips 2012]

Table 1: Input Dataset Used for Model Development [Philips 2012]

	Current	T_s	CCT
Test1	0.35A	55°C	3000K
Test2	0.35A	85°C	3000K
Test3	0.35A	105°C	3000K
Test4	0.35A	120°C	3000K
Test5	0.5A	55°C	3000K
Test6	0.5A	85°C	3000K
Test7	0.5A	105°C	3000K
Test8	0.5A	120°C	3000K
Test9	0.7A	55°C	3000K
Test10	0.7A	85°C	3000K
Test11	0.7A	105°C	3000K
Test12	1A	55°C	3000K
Test13	1A	85°C	3000K
Test14	1A	105°C	3000K

Table 2: LED Surface Temperature for Various Ambient Temperatures [Philips 2012]

Ambient Temperature	Surface Temperature
55°C	53°C
85°C	83°C
105°C	103°C
120°C	118°C

Failure Mechanisms

The observed lumen degradation in the LEDs may categorized into two main categories including, (1) wear-out resulting from long term degradation, (2) catastrophic failure of the LED resulting from short term degradation (Figure 2). Catastrophic short term degradation may be caused by manufacturing problems, operation problems, harsh environment exposure or other unpredicted elements in the LED system. Long term degradation may be caused by long-term exposure to harsh environments can be represented by a simple ramp function decay, polynomial function family decay, exponential family decay, or complicated and combined functions to model statistical model family decay. In this paper, we mainly focus on the long term degradation of Lumen Maintenance, from which the wearing life of LEDs is predicted.

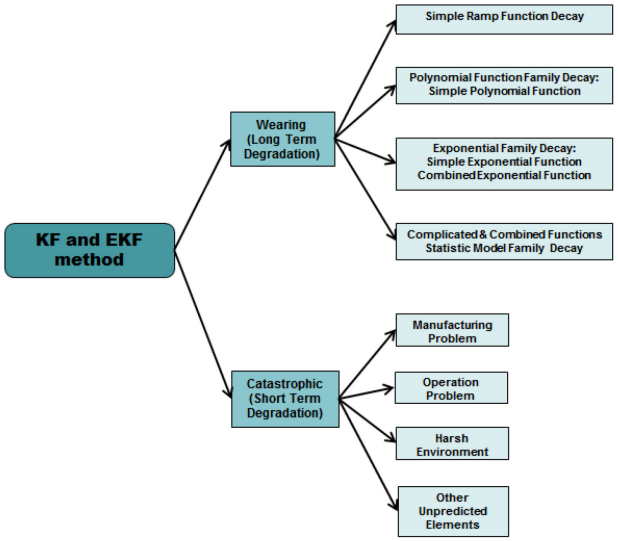

Figure 2: LEDs Failure Categories

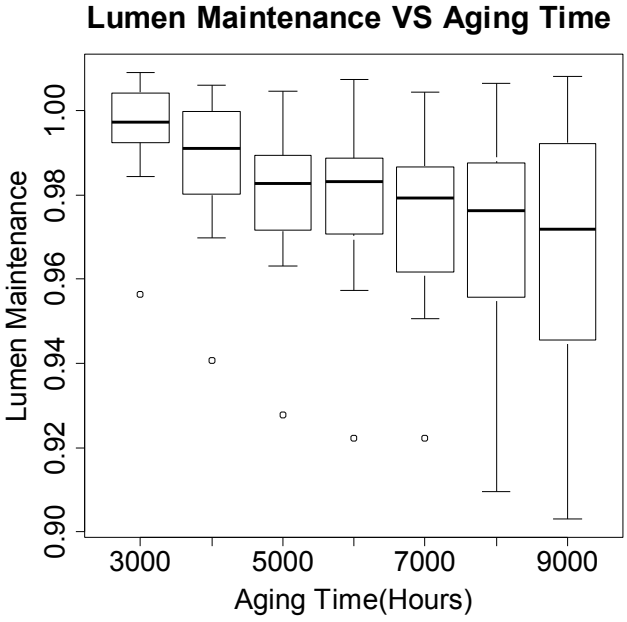

Figure 3: Distribution for the Experimental Dataset

Analysis of the variance in the lumen output from the LED versus lifetime at high temperature shows that the variance in the LED output increases with the increase in operating time at high temperature. Simple regression of the test data versus test time indicates that the lumen maintenance mean of the tested distribution oscillates with respect to test time. However, majority of the test data falls within the ±95% confidence limits.

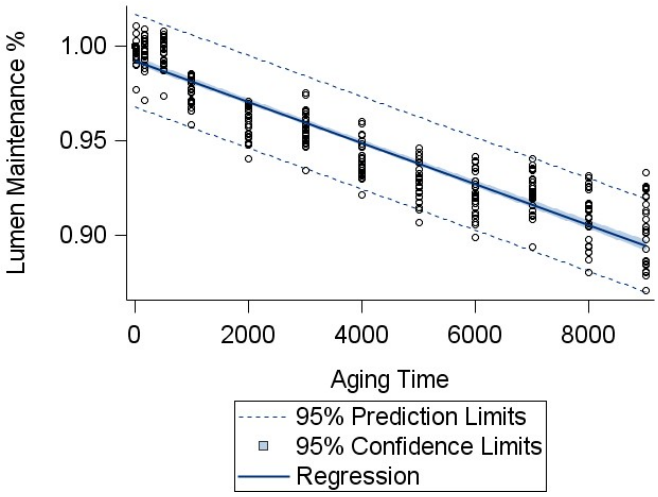

Figure 4: Simple Regression for the Experimental Dataset

Degradation in the LED after exposure to harsh environments may cause a shift in the correlated color temperature (CCT). The color may shift from blue to orange or from green to pink or vice-versa. There are a number of reasons for the color shift including (1) aging of the LEDs, or UV exposure may cause plastics to change color (2) operating conditions including contaminants in the atmosphere may cause luminaire changes (3) light engines may shift color over time with different engines shifting in color differently, (4) maintenance issues may cause the luminaires to look different over time due to a number of reasons including incorrect installation of parts. Nearly all the light engines have some type of color shift. Examples include (1) metal halide lamps which are notorious for color shift (2) incandescent bulbs color shift when they are dimmed (3) LEDs that will shift color over time. While, linear fluorescents may not color shift "much" however, improper maintenance practices can cause obvious luminaire color shift over time. The causes of color shift with LEDs are not well understood. The color shift in LEDs needs specific attention for a number of reasons. Prior testing has shown that the color shift with LED-based luminaires can be so great as to constitute a "failure" to an end user. In this paper, Extended Kalman Filter has been used to project color shift over an extended period of time.

Chromaticity specifies the quality of color regardless of the luminance and is quantified by the hue and saturation. The white point of the illuminant is the neutral reference. The white point of an RGB display is the x,y chromaticity of [1/3, 1/3]. All other chromaticities are described in relation to this white point reference using polar coordinates. Hue is the

angular component and saturation or purity is the radial component. The outer curved boundary of the chromaticity diagram is the spectral or monochromatic locus, with wavelengths shown in nanometers. The "horseshoe" shape of the chromaticity diagram consists of the (x,y) chromaticity points of every color of light whose spectrum consists of only

a single wavelength. Chromaticities that lie along the horse shoe are called spectral chromaticities. Colors along the horse

show range from violet, magenta, blue, cyan, green, yellow and red. The dotted line at the bottom of the chromaticity diagram completes the region "enclosed" by the horseshoe. The chromaticities along the straight line are not "spectral" and there is no light with only a single wavelength component that exhibits a color with such a chromaticity. Colors along the straight line are called the nonspectral purples.

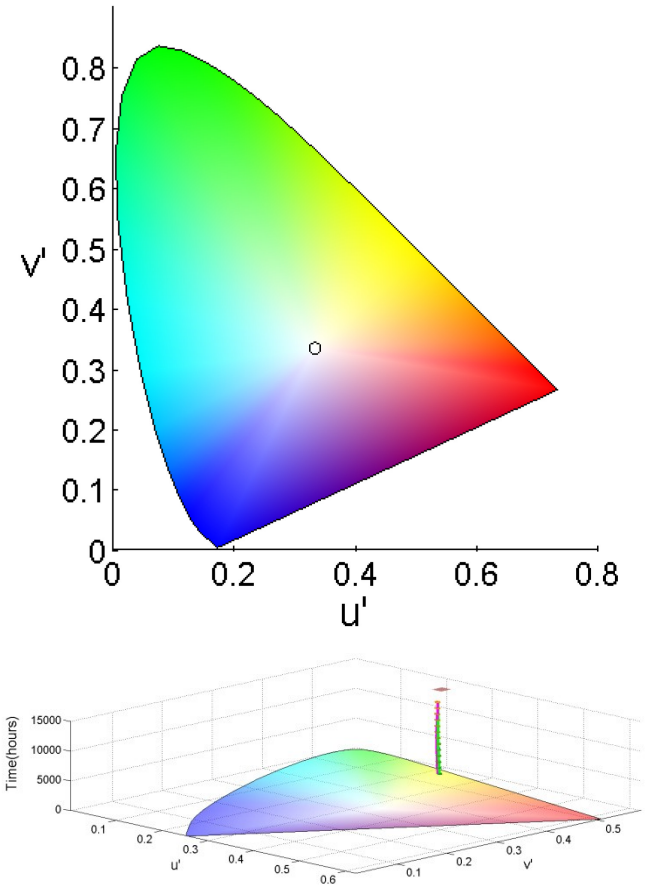

Figure 5: Yu'v' is a uniform luminance-chrominance space and the visualized color of 3000K using 1976CIEUV and Location of the 55°C, 0.35A dataset

Color space is a three-dimensional space in which the color is specified by a set of three numbers such as the CIE coordinates X, Y, and Z, which specify the color and brightness. The CIE XYZ color space is designed so that the Y parameter is a measure of the brightness or luminance of a color. The chromaticity is a color projected into a two-dimensional space that ignores brightness. The chromaticity

$$x = \frac{X}{X+Y+Z} \quad (1)$$

$$y = \frac{Y}{X+Y+Z} \quad (2)$$

$$z = \frac{Z}{X+Y+Z} = 1 - x - y \quad (3)$$

Where, Y means luminance, Z is equal to blue stimulation, or the S cone response, and X is a linear combination of cone response curves chosen to be nonnegative. The XYZ tristimulus values are derived parameters from the long-, medium-, and short-wavelength cones. The Y luminance is measured in foot-Lamberts or candelas/sq.m, and the x and y co-ordinates are dimensionless. The derived color space is specified by x, y, and Y and is known as the CIE xyY color space and is widely used to specify colors in practice. The Yu'v' is a uniform luminance-chrominance space. Yu'v' is derived from XYZ space [CIE 1986; Poynton 2003],

$$u' = \frac{4X}{X+15Y+3Z} = \frac{4x}{-2x+12y+3} \quad (4)$$

$$v' = \frac{9Y}{X+15Y+3Z} = \frac{9y}{-2x+12y+3} \quad (5)$$

In the experimental data-set, the initial CCT of warm LUXEON LED value is 3000K whose u' and v' location in 1976 CIE [Schanda 2007] is shown in the following Figure 5. The vertical stack of points indicates the (u', v') coordinates of all the data at 55°C, 85°C and 105°C from pristine state till 10,000 hours of testing.

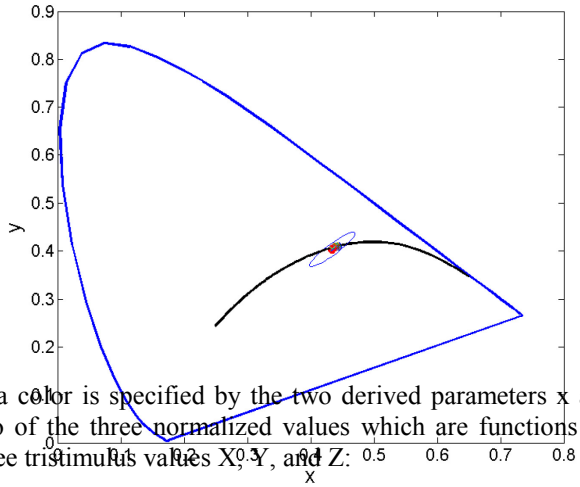

of a color is specified by the two derived parameters x and y, two of the three normalized values which are functions of all three tristimulus values X, Y, and Z:

Figure 6: Planckian Locus in Yxy CIE1931XY Space and Location of the 55°C, 0.35A dataset.

Planckian locus, also called the black body locus is the path that the color of an incandescent black body would take in a particular chromaticity space as the blackbody temperature changes. The blackbody goes from deep red at low temperatures through orange, yellowish white, white, and finally bluish white at very high temperatures. Figure 6 shows the Planckian Locus in the Yxy space (Black Line). The red- dot on the Planckian Locus indicates the location of the 55°C

ambient air, 1A test data set. The data-set consists of 26-samples and has a mean CCT of 2952K. The (u', v') data from experiments has been converted to the (x, y) space and plotted in Figure 6 [Poynton 2003].

$$x = \frac{9u'}{6u' - 16v' + 12} \quad (6)$$

$$y = \frac{4v'}{6u' - 16v' + 12} \quad (7)$$

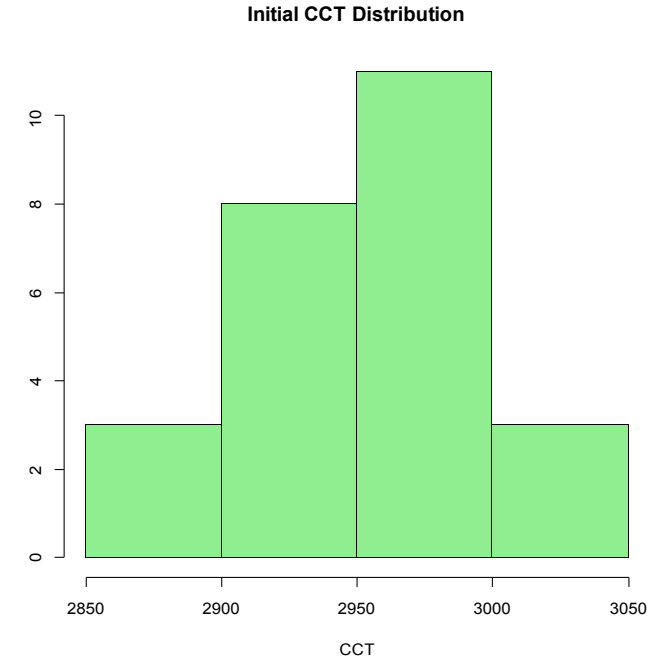

Figure 7: Variance of the CCT in the 55°C, 0.35A Dataset

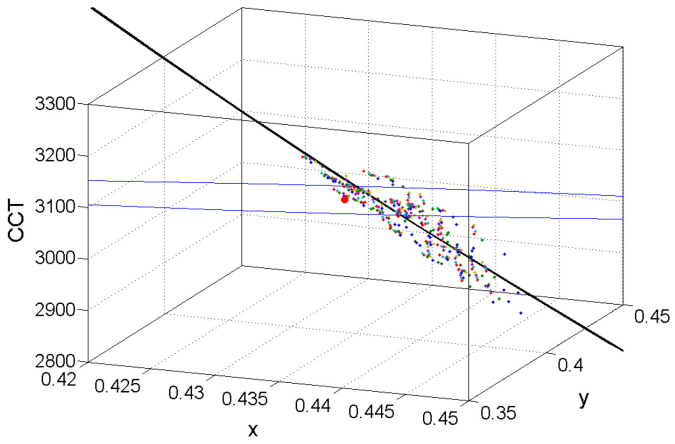

Figure 8: Evolution of the CCT for the 55°C, 0.35A Data-set along the Planckian Locus with Test Time up to 10,000 Hours in Yxy CIE1931 Space

One can approximate the Planckian locus in order to calculate the CCT in terms of chromaticity coordinates, if a narrow range of color temperatures is considered, such as those encapsulating daylight. The cubic approximation proposed by McCamy [1992] has been used to construct the Planckian Locus,

$$CCT(x, y) = -449n^3 + 3525n^2 - 6823.3n + 5520.33 \quad (8)$$

$$n = \frac{x - x_e}{y - y_e} \quad (9)$$

Where, n is the inverse slope in the x-y space, $x_e = 0.3320$, and $y_e = 0.1858$. Variance of the CCT in the experimental data is shown in Figure 7. LEDs subjected to high temperature exposure shift in the 1976CIEUV space with accelerated test time. Figure 9 shows the u' and v' coordinates for the data-set and the dataset mean versus operating hours. The red line is the average of 55°C chromaticity, the blue line is average of 85°C chromaticity, the green line is average of 105°C chromaticity and the pink line is average of 120°C chromaticity. It is thus expected that the color would shift with time of exposure at high temperature.

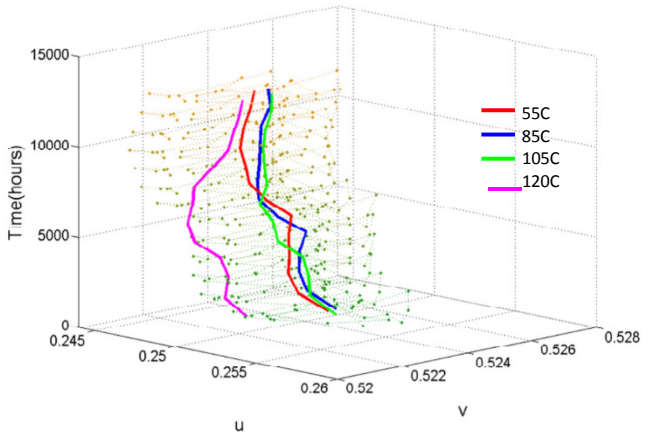

Figure 9: Shift of the LED Chromaticity in the CIE1976UV space. Plot depicts the change in (u', v') for the different temperatures versus test time in hours. Plotted data corresponds to current of 0.35A.

Extended Kalman Filter Based Assessment of L70 Life

In order to prognosticate the remaining useful life (RUL) of LEDs, the L70 lifetime has been used. The L70 life is defined as the time at which LED lumen output is 70 percent of the lumen output compared to the pristine LED at beginning of the test.

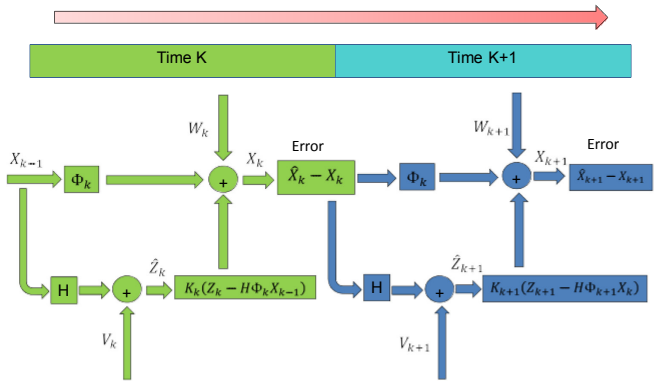

Figure 10: Recursive Algorithm and Extended Kalman Filter

The RUL is estimated by the using the Extended Kalman Filter with historic data. System damage state estimation in the presence of measurement noise and process noise has

been achieved using the Extended Kalman Filter (EKF).

Previously, the Kalman Filter has been used in guidance and tracking applications [Kalman 1960, Zarchan 2000]. System state has been described in state space form using the measurement of the feature vector, velocity of feature vector change and the acceleration of the feature vector change. The equivalent Extended Kalman Filter equation for state space

representation is in the presence of process noise and measurement noise is:

$$\dot{x}=Fx+w \tag{10}$$

$$\dot{x}=f(x)+w \tag{11}$$

Where the F is the system linear dynamic matrix; f(x) is non-linear dynamic matrix; the G is measurement matrix; u is measurement vector; and w is system white noise;

$$Z=H\cdot x+V \tag{12}$$

$$Z=h(x)+V \tag{13}$$

Where H is the measurement matrix, z is the measurement vector, h(x) is a measurement function,which is a nonlinear function of states, v is zero-mean random process described by the measurement noise matrix. The process noise can be calculated by taking the expected value of white noise:

$$Q=E[ww^T] \tag{14}$$

Similarly, the measurement noise matrix is derived from the measurement noise as following:

$$R=E[vv^T] \tag{15}$$

Since the system-dynamics 'F' and measurement equations are nonlinear, a first-order approximation is used in

the continuous Riccati equations for the systems dynamics matrix F and the measurement matrix H. It is expected that the progression of interconnect damage is nonlinear, and

therefore need to be linearized before it can be estimated. In the Extended Kalman Filter, the problem of linearization is

addressed by calculating the Jacobian of the nonlinear function of states (f) and the measurement function (h) around

the estimated state. System state at each future time has been

computed based on the state space at preceding time step, system dynamics matrix, control vector, control matrix,

measurement matrix, measured vector, process noise and measurement noise. The matrices are related to the nonlinear

system and measurement equations according to:

$$F=\left.\frac{\partial f(x)}{}\right| \tag{16}$$

The system dynamic matrix for the EKF is:

$$F_{EKF}=\begin{bmatrix} \frac{\partial \dot{x}}{\partial x} & \frac{\partial \dot{x}}{\partial \dot{x}} & \frac{\partial \dot{x}}{\partial b} \\ \frac{\partial \ddot{x}}{\partial x} & \frac{\partial \ddot{x}}{\partial \dot{x}} & \frac{\partial \ddot{x}}{\partial b} \\ \frac{\partial \dot{b}}{\partial x} & \frac{\partial \dot{b}}{\partial \dot{x}} & \frac{\partial \dot{b}}{\partial b} \end{bmatrix} \tag{19}$$

The system dynamic matrix for the KF is:

$$F_{KF}=\begin{bmatrix} 0 & 1 & 0 \\ 0 & 0 & 1 \\ 0 & 0 & 0 \end{bmatrix} \tag{20}$$

We use this Jacobin Matrix to linearize the non-linear problem; therefore it can use the classical KF updates. This is for the second order system, and thus we can find the transfer

function F to describe certain system, which it is the key to find fundamental matrix $\Phi(t)$. In this paper for the EKF, we

used the system model:

$$x=\alpha\cdot e^{\beta\cdot t} \tag{21}$$

The state vector is:

$$x_k=\begin{bmatrix} x & \dot{x} & \beta \end{bmatrix} \tag{22}$$

This is an exponential function. The 'α' and 'β' are two

coefficients that are decided by different systems. The first derivation $\dot{x}$and the second derivation $\ddot{x}$are from:

$$x=\alpha\cdot e^{\beta\cdot t} \tag{23}$$

$$\dot{x}=\beta\cdot x \tag{24}$$

$$\ddot{x}=\beta\cdot\dot{x}=\beta^2\cdot x \tag{25}$$

Therefore the elements in system dynamic matrix will be calculated as:

$$F_{EKF}=\begin{bmatrix} \beta & 1 & x \\ \beta^2 & \beta & 2\beta x \\ 0 & 0 & 0 \end{bmatrix} \tag{26}$$

Usually, the fundamental matrix $\Phi(t)$ can be obtained from

two ways: the first way, we can get it from Laplace Transform, simply as:

$$\Phi(t)=\ell^{-1}[(SI-F)^{-1}] \tag{27}$$

Where the ℓ^{-1} is inverse of the Laplace Transform; However, the second way, known as the common way to find $\Phi(t)$, derives from the Taylor Series expansion:

$$\partial x \Big|_{x=\hat{x}}$$

$$H = \frac{\partial h(x)}{\partial x}\Big|_{x=\hat{x}} \tag{17}$$

From the linear dynamic equations, we can clearly know that the world is linear as we supposed, and once we made this premise. All the problems can be simply solved through the matrix calculation. Therefore, we can get the first and second derivatives from the linear matrix calculation;

$$\begin{bmatrix} \dot{x} \\ \ddot{x} \end{bmatrix} = F \cdot \begin{bmatrix} x \\ \dot{x} \end{bmatrix} \tag{18}$$

$$\Phi(t) = I + FT + \frac{(FT)^2}{2!} + \frac{(FT)^3}{3!} + \cdots \tag{28}$$

Normally, we only use the first two terms for representing the fundamental matrix $\Phi(t)$, because the adding more terms cannot contribute much to the precision and filter convergence.

The Fundamental Matrix in the Extended Kalman Filter is:

$$\Phi_{EKF}(T) \approx I + F_{EKF}T = \begin{bmatrix} 1+\beta T & T & xT \\ \beta^2 T & 1+\beta T & \\ & & 2\beta \cdot xT \\ 0 & 0 & 1 \end{bmatrix} \tag{29}$$

The Fundamental Matrix in the Extended Kalman Filter is:

$$\begin{bmatrix} 1 & T & 0.5Ts^2 \end{bmatrix} \tag{30}$$

$$\Phi_{KF}(T) \approx I + F_{KF}T = \begin{bmatrix} 0 & 1 & T \\ 0 & 0 & 1 \end{bmatrix}$$

In the Kalman Filter, the Fundamental Matrix will be directly used to update the estimation from last time to the next. Generally speaking, the process to find the ideal estimation can be expressed as following steps: First of all, we make the primary estimation, which should be approximate to the initiate value in the dataset, and secondly, we can find the first projection using the fundamental matrix $\Phi(t)$ and simply calculate as:

$$\bar{x} = \Phi(t) \cdot \hat{x} \tag{31}$$

For the KF the projection can be represented by:

$$\begin{bmatrix} \Delta\dot{x} \\ \Delta\ddot{x} \\ \Delta\dot{x} \end{bmatrix} = \begin{bmatrix} 0 & 1 & 0 \\ 0 & 0 & 1 \\ 0 & 0 & 0 \end{bmatrix} \begin{bmatrix} \Delta x \\ \Delta\dot{x} \\ \Delta\ddot{x} \end{bmatrix} + \begin{bmatrix} 0 \\ 0 \\ w \end{bmatrix} \tag{32}$$

For the EKF the projection can be represented by:

$$\begin{bmatrix} \Delta\dot{x} \\ \Delta\ddot{x} \\ \Delta\dot{b} \end{bmatrix} = \begin{bmatrix} \Delta x & \Delta\dot{x} & \Delta b \\ \Delta\ddot{x} & \Delta\ddot{x} & \Delta\ddot{x} \\ \overline{\Delta x} & \overline{\Delta\dot{x}} & \overline{\Delta b} \end{bmatrix} \begin{bmatrix} \Delta x \\ \Delta\dot{x} \\ \Delta b \end{bmatrix} + \begin{bmatrix} 0 \\ 0 \\ w \end{bmatrix} \tag{33}$$

$$\begin{bmatrix} \overline{\Delta\dot{x}} & \overline{\Delta\dot{x}} & \overline{\Delta\dot{x}} \\ \Delta\dot{x} & \Delta\dot{x} & \Delta\dot{x} \\ \Delta\dot{b} & \Delta\dot{b} & \Delta\dot{b} \end{bmatrix}$$

The next estimate could be obtained from the following equation:

$$\hat{x} = \bar{x} + K(Z - H \cdot \bar{x}) \tag{34}$$

K is Kalman Gain

H is measurement matrix

Z is measurement.

Each time we update the Kalman Gain and Covariance Matrix, which minimizes the errors and makes optimal calculation during each step. Thus, the Kalman Gain mainly conveys the information about how is our estimation close to the observation. The way to obtain Kalman Gain (K) is from three Riccati equations:

the H is the unit measurement matrix and H_t is transpose of it; the K is the Kalman Gain; R_k represents the measurement noise according to the different system. We notice that those three equations run like in the recursions: for the initial covariance error P_0, we can find variance matrix M_k that represents the current error in the first equation according to time. Then we use it in the second equation to find the Kalman Gain K, after that, we substitute the Estimate Kalman Gain K into the third equation to update last covariance error P_k, thus we obtain the 'next' covariance error P_{k+1}. Therefore, as we go back to the first equation, we can obtain the updated M_k and updated Kalman Gain K. In the EKF, the Euler integration has been introduced to instead the performance of the KF's fundamental matrix, it can be found that:

$$\bar{x}_k = \hat{x}_k + \dot{\bar{x}}_{k-1} T \tag{40}$$

$$\dot{\bar{x}}_k = \hat{\dot{x}}_k + \ddot{\bar{x}}_{k-1} T \tag{41}$$

We call the equation above is the update equations, $\hat{x}_k$ represents the projection from the last time k ; $\hat{\dot{x}}_{k-1}$ is the first derivative at time k-1; $\hat{x}_k$ is the estimation at time k, $\dot{x}_k$ is the first derivative at time k; T is the sample time.

$$\hat{x}_k = x_k + K_1(Z - H \cdot x_k) \tag{42}$$

$$\hat{\dot{x}}_k = \dot{x}_k + K_2(Z - H \cdot x_k) \tag{43}$$

The above equations are the basic Extended Kalman Filter equations, which are to find the estimation and its 'velocity'. Also, in those equations, it uses the same three Riccati Equations that expressed in the Kalman Filter to obtain the Kalman Gain K_1 and K_2. Thus, the Extended Kalman Filter actually has turned the non-linear problem into a linear one through integrating method. So at each step, the Extended Kalman Filter made a small integration, and if the integrate time is small enough, then the answer we get is becoming more precise. However, the difficulty within the Extended Kalman Filter is to find the dynamic non-linear model to describe the system, which always contains the unknown coefficients. Therefore, the better we know about the test

$$M_k = \Phi_k P_k \Phi_k{}^T + Q_K \quad (35)$$

$$K = M_k H_t (H M_k H_t + R_k)^{-1} \quad (36)$$

$$P_k = (I - KH) M_k \quad (37)$$

In the above equations, the M_k is the covariance matrix; the Φ is the fundamental matrix; the Φ^T is the transpose of that matrix; P_k is another covariance matrix that representing error according to the time; the Q_k is the discrete process noise matrix, which is calculated from:

$$Q = \Phi_s \begin{bmatrix} 0 & 0 & 0 \\ 0 & 0 & 0 \\ 0 & 0 & 1 \end{bmatrix} \quad (38)$$

$$Q^k = \int_0^{Ts} \Phi(\tau) \cdot Q \cdot \Phi(\tau)^T d\tau \quad (39)$$

system, for example, the theories and functions in the situation of LEDs failure, the better we can predict system model in the Extended Kalman Filter, therefore, the prediction of Remaining Useful Life (RUL) would be close to the real RUL in our PHM.

Algorithm: Filtering and RUL prediction

1. Initiate $\hat{x}_0$
2. Make the projections:

   $\bar{x}_k = \hat{x}_k + \dot{x}_{k-1} T$

   $\bar{\dot{x}}_k = \hat{\dot{x}}_k + \ddot{x}_{k-1} T$
3. Calculate error covariance matrix before updata:

   $M_k = \Phi_k P_k \Phi_k{}^T + Q_K$
4. Calculate the Kalman Gain:

   $K = M_k H_t (H M_k H_t + R_k)^{-1}$
5. Update the estimation with measurement:

$$\hat{x}_k = \bar{x}_k + K_1(Z - H \cdot \bar{x}_k)$$

$$\hat{\dot{x}}_k = \bar{\dot{x}}_k + K_2(Z - H \cdot \bar{x}_k)$$

6. Calculate error covariance after measurement update: $P_k = (I - KH)M_k$
7. Extrapolate feature vector to threshold value:

$$LM = \bar{x}_{k+n} \cdot e^{\bar{\beta}_{k+n}} + w_{k+n}$$

8. Report predicted RUL (and uncertainty);
9. Iterate to step 2 for next measurement (k = k +1);

The predictions are updated continually as more data becomes available. The Figure 11 below shows the estimation of RUL for L70. In the plot the blue line is raw experimental dataset, the solid red line is Extended Kalman Filter Prediction, and the dash red line is Extended Kalman Filter extrapolations for L70, the green line is L70 criterion, and the green arrow shows the Remaining Useful Life from the last evaluated point.

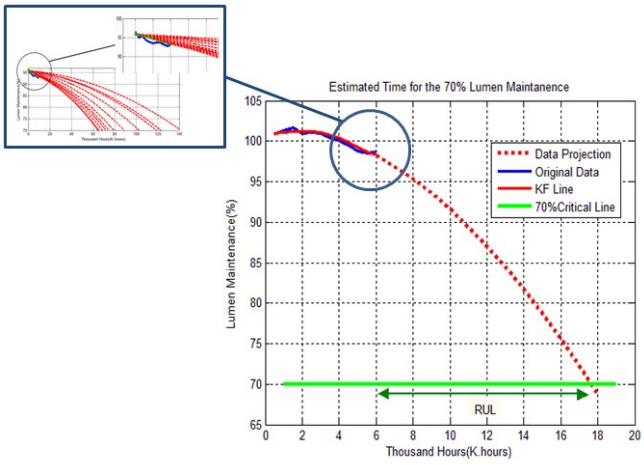

Figure 11 the Intuition of RUL for L70

Different failure models have been integrated with the Extended Kalman Filter Algorithm to extrapolate the pseudo decay curve, and calculate the Remaining Useful Life using L70 criterion. The extrapolation function uses state vectors from Extended Kalman Filter estimations. The state vectors provide information about the migration of accrued damage in the LED. Once all the state vectors converge at certain level, the Extended Kalman Filter prediction of decay lines will converge and remain within 95-percent Confidence Interval level.

TM-21 Estimation of LED Life

$$\log_e(\Phi(t)) = \log_e(\beta) + (-\alpha) \cdot t \quad (45)$$

$$\bar{\Phi} = \bar{\beta} + \bar{\alpha} \cdot \bar{t} \quad (46)$$

Coefficients of regression have been computed to get the optimal curve fit for the 'slope' and 'intercept'. The values of $\alpha$and βwere determined for the lower case temperature T1, and for the upper case temperature T2.

$$\bar{\alpha} = -\alpha = \frac{N\left(\sum_{i=1}^{N} t_i \cdot \Phi(t)_i\right) - \left(\sum_{i=1}^{N} t_i\right)\left(\sum_{i=1}^{N} (\Phi(t)_i)\right)}{N \cdot \sum_{i=1}^{N} t_i^2 - \left(\sum_{i=1}^{N} t_i\right)^2} \quad (47)$$

$$\bar{\beta} = \log(\beta) = \frac{\left(\sum_{i=1}^{N} \Phi(t)_i\right) - \alpha \cdot \left(\sum_{i=1}^{N} t_i\right)}{N} \quad (48)$$

Activation Energy was calculated using the decay rate from two different temperatures:

$$E_a = \frac{k \cdot \log\left(\frac{\alpha_2}{\alpha_1}\right)}{\left|\frac{1}{T_2} - \frac{1}{T_1}\right|} \quad (49)$$

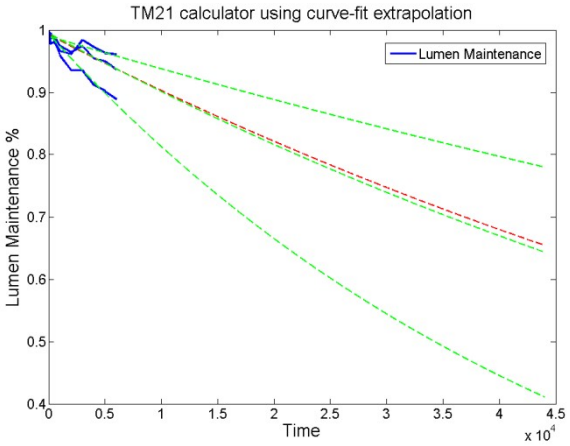

Figure 12: TM-21 Degradation Curve

Using the activation energy E_a and the lower case αvalue and temperature, the Pre-Exponential Factor A, was determined.

$$A = \alpha \cdot e^{\frac{E_a}{k \cdot \left|\frac{1}{T_1}\right|}} \quad (50)$$

With the Pre-Exponential Factor known, the In-Situ temperature αvalue was determined.

Computation method based on TM-21 includes four parts: the first part uses the Least Squares Fit (LSF) to determine the Projected Initial Constant α and Decay Rate Constant β, The governing function for the Lumen Maintenance according to time:

$$\Phi(t) = \beta \cdot e^{-\alpha \cdot t} \tag{44}$$

The lumen maintenance, $\Phi(t)$, is known for about a dozen datum points. In order to solve for α and β, the logarithm of both sides was taken to produce a linear function.

$$\alpha = A_0 \cdot e^{\left(\frac{E_a}{k \cdot T_1}\right)} \tag{51}$$

Next, the In-Situ temperature β value was determined.

$$\beta_0 = \sqrt{\beta_1 \cdot \beta_2} \tag{52}$$

Lastly, with the values of α and β known for the In-Situ temperature, the L70 value in hours was determined.

$$L_{70} = \frac{\log\left(\frac{\beta}{0.7}\right)}{\alpha_0} \quad (53)$$

The TM-21 extrapolation curve is shown in Figure 12. The green dash lines are the extrapolations from the low temperature to the high temperature. The red dash line shows the overall lumen degradation. The L70 life of LED using TM-21 is about 36871.4 hours for long-term degradation. However there is a limitation to use this TM-21 Calculator, we have to know at least three cases at different temperatures in order to correctly calculate the Activate Energy Ratio. Moreover, the TM-21 is single estimation value, which cannot provide any insight into the Probability and Distribution of L70 estimations.

EKF Model Analysis

General LED Lumen Decay Life-Prediction functions are plotted in Figure 13 and shown in Table 3. Potential failure mechanisms in the LED system include: (1) Silicone Encapsulate Degradation; (2) Chip Degradation; (3) Phosphor Degradation; (4) Reflector Degradation; and (5) Glass Degradation.

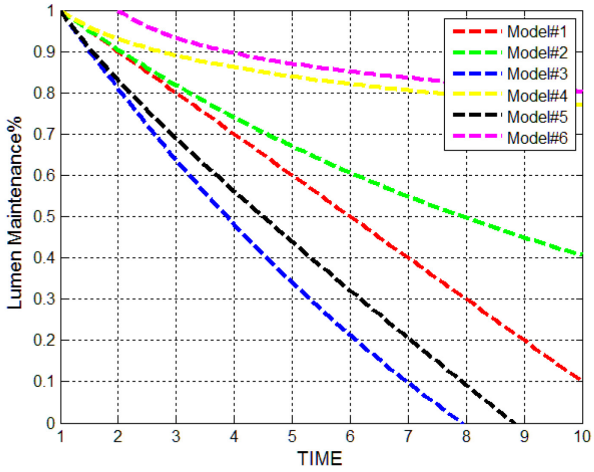

Figure 13: LED Lumen Decay models

Table 3: Lumen Decay Models [IES TM-21 2011]

	Model
Model-1	$I_v = I_v^0 + K_1(t - t^0)$
Model-2	$I_v = I_v^0 \exp\left[k_2\left(t - t^0\right)\right]$
Model-3	$I_v = \left(I_v^0 + \frac{k_1}{k_2}\right)\exp\left[k_2\left(t - t^0\right)\right] - \frac{k_1}{k_2}$
Model-4	$I_v = I_v^0 + k_3 \ln\left(\frac{t}{t^0}\right)$
Model-5	$I_v = I_v^0 + k_1\left(t - t^0\right) + k_3 \ln\left(\frac{t}{t^0}\right)$
Model-6	$I_v = I_{v0}\left(t - t^0\right)^{k_5}$

Each failure mechanism may have different underlying failure physics and a different unique function to describe it. The following plot shows the possible decay models existing in the LED systems. The overall degradation in LED Lumen Maintenance may result from several combined long term decay functions triggered by multiple failure mechanisms. Thus, the true lumen degradation profile may be fairly complicated. In this paper, we primarily focus on three failure mechanisms. The first failure mechanism is the drift of charged defects in chip, which may be described as the ramp function [IES TM21 2011]. The second failure mechanism is thermal decomposition of encapsulant, which is represented as an exponential function. The third failure mechanism is the combination of those previous two models. Figure 14 shows the constant decay rate model for the prediction of the Pseudo L70 life for the LEDs. The charge drift model model is described by the function:

$$dL_o / dt = C_1 \quad (54)$$

$$L_o = L_1 + C_1(T - T_0) \quad (55)$$

In this model, the decay rate is constant, which is presented by the straight lines (Figure 14). Constant degradation rate cannot truly describe the degradation in operational environments, where the decay rate may not be maintained constant throughout the LED Lifetime.

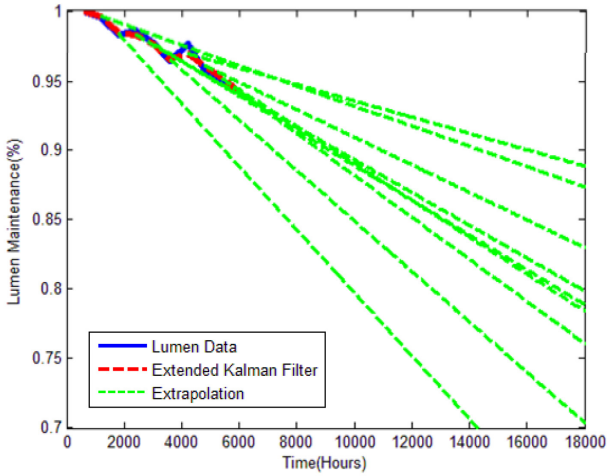

Figure 14: Constant Decay Model with Kalman Filter for L70 Estimation of 105°C, 1A LEDs

Initial stages of lumen degradation in LEDs may result from chip degradation or plastic degradation. However, as the time elapses, the damage evolution in the system may include additional failure mechanisms and thus additional lumen degradation trends. It is feasible for several failure mechanisms working together to accrue the damage and accelerate failure of system. In order to allow evolution of damage at a non-constant decay rate, a second order polynomial function has been incorporated into the extended Kalman filter algorithm to predict decay curve (Figure 15). Figure 15 shows the accelerating degradation using the polynomial function where the decay rate is not constant, which expresses as:

$$dL_o / dt = C_1 + C_2 T$$

$$_{o} = L_I + C_1(T \quad (56)$$

$$-T_0) + 0.5C_2 \quad (57)$$

$$(T - T_0)$$

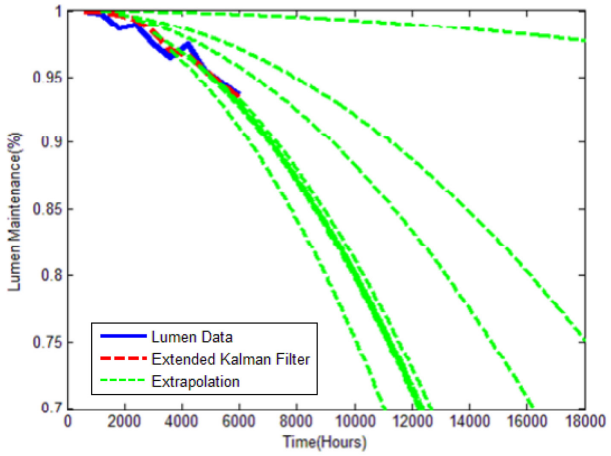

Figure 15: Polynomial Decay Model with Kalman Filter for L70 Estimation of 105°C, 1A LEDs

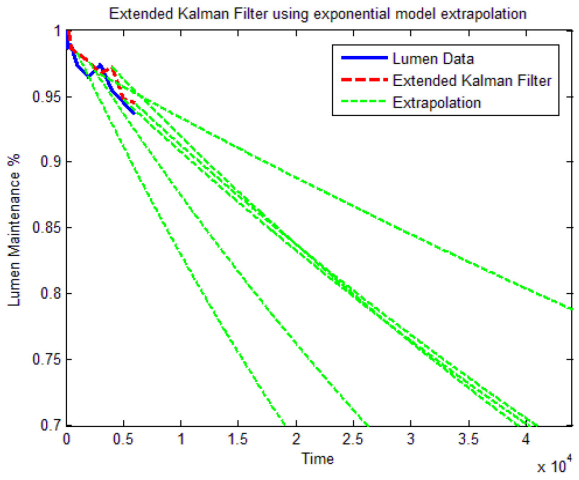

Figure 16: Exponential Decay Model with Kalman Filter for L70 Estimation of 105°C, 1A LEDs

Further, the LED system may experience long-term degradation in high temperature environments. In this case, the main degradation in the system may result from thermal decomposition of encapsulant in LEDs. In this case, the exponential decay function is used to represent the decay curve in the extended Kalman filter algorithm. This extrapolation is presented in the Figure 16 and represented by,

$$dL_o / dt = C_1 \times L_0 \tag{58}$$

$$L_o = L_I \times e^{C_1 \times (T - T_0)} \tag{59}$$

L70 Life Distribution Using KF and EKF

Exponential decay function (Model 3) has been used to predict the L70 life. Extended Kalman filter has been used to estimate the L70 life of each LED based on prior measured values of lumen maintenance. Figure 17 shows the EKF prediction of L70 life depicted by red-lines for each sample in the 105°C, 1A experimental dataset. The degree of correlation between the measured data and the EKF predictions of state can be assessed by comparing the red- lines for EKF predictions with the actual measurements of lumen output indicated by the blue-dots for each of the 25 samples in the measured sample-set. In each case, the pseudo

L70 life has been estimated using EKF in conjunction with the Newton Raphson Method. When Kalman Filter made a prediction about the state vectors in each evaluated time, and the remaining useful life could be estimated and calculated mathematically by solving the equation H(t) and find the time T-prediction:

$$H(t) = x_0 + \dot{x} \times t + \ddot{x} \times t^2 - f(EoL) \tag{60}$$

$$T(n+1) = T(n) - f(x) / f'(x) \tag{61}$$

Where, $T(n)$ is the estimated root at time n; $T(n+1)$ is the estimated root at time (n+1); $f'(x)$ is the derivation of target equation. The Predicted RUL (T-predicted) is known as the 'L70' End of Life (EoL) minus the sampling time (T-sample). So the algebra equations presents as following:

$$RUL = L70_{EKF} - T_{sample} \tag{62}$$

Coefficients for the estimation for the exponential model ($\Phi = \alpha \cdot \exp(-\beta \cdot t)$) used with extended Kalman filter have been computed by training the EKF parameters in the prior acquired data. In this model, Φ is the Lumen Maintenance (%), α is the initial degradation factor, β is the degradation rate. The estimation parameters α_i and β_i are shown in Figure 18 and Figure 19.

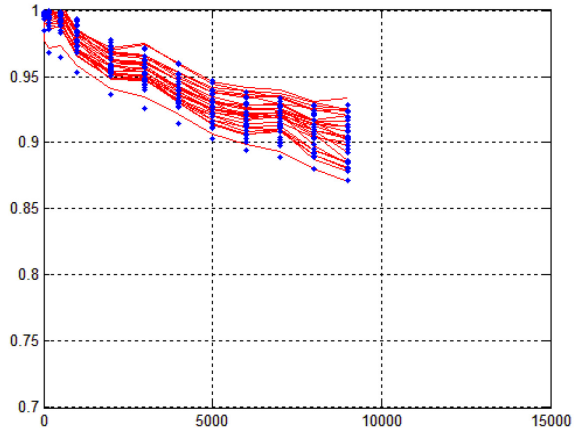

Figure 17: KF Estimations

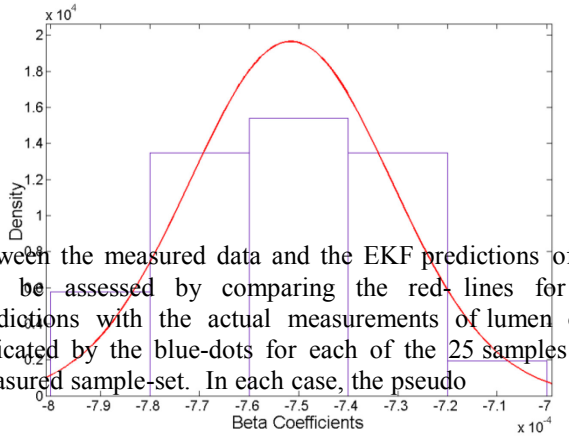

Figure 18: Fitted Distribution for Decay Rate β_i after 8000 hours for 105°C, 1A dataset.

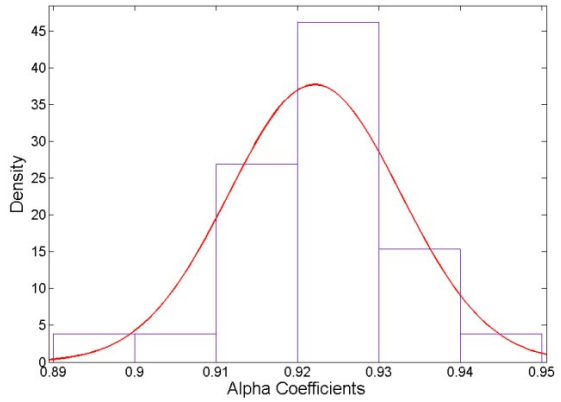

Figure 19: Fitted Distribution for Decay Rate α_i after 8000 hours for 105°C, 1A dataset.

Figure 20 shows the KF predictions of L70 life with the green lines using exponential model. Those extrapolation lines have been drawn by the coefficients estimated by the KF in the above table. The blue line in the picture shows the true estimation, which is the mean of the distribution; the red curve shows the variance of the distribution.

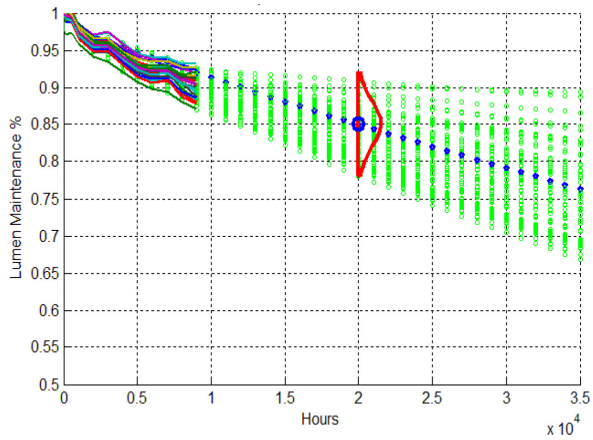

Figure 20 EKF Extrapolations and Mean Estimations

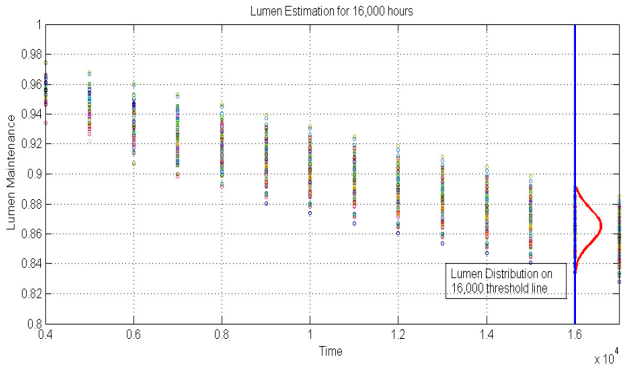

Figure 21 Lumen Degradation Path for estimating lumen at 16,000 hours

Using the presented approach, the lumen degradation could be predicted at future time. Figure 21 shows the prediction of Lumen Maintenance at 16,000 hours using EKF. Normal distribution has been assumed for the estimation of training decay rates. Figure 21 shows the degradation path for estimating the 16,000 hours life. The dots represent the lumen maintenance estimations, and the blue line shows the 16,000 hours threshold.

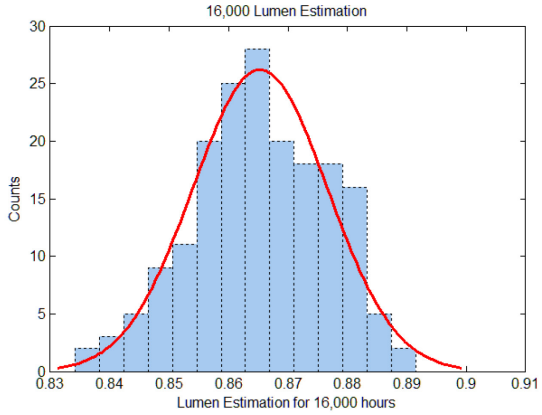

Figure 22 Lumen Estimation Summary for 16,000 hours

Figure 22 shows the lumen estimation at 16,000 hours. The blue bar shows the counts of estimated lumen value, the red line is fitted distribution. The mean value of 16,000 hours lumen maintenance is 86.53%, and the mean value of 8000 hours is 92.21%. Therefore, the lumen maintenance degradation from 8000 hours to 16,000 hours is 5.68 %. The lumen maintenance variance at 8000 hours is 1.1196e-04, and the lumen maintenance variance at 16,000 hours is 1.2863e-04, so the variance increases 1.667e-5, which indicates the distribution shape is wider than the distribution at 8000 hours.

KF Chromaticity Tracking Using EKF

The Chromaticity u' and v' has also been tracked by the Kalman Filtering Algorithm (Figure 23). Predictions of Chromaticity shift along with lumen maintenance can provide valuable insight in to the prior damage and the remaining useful life of the LEDs.

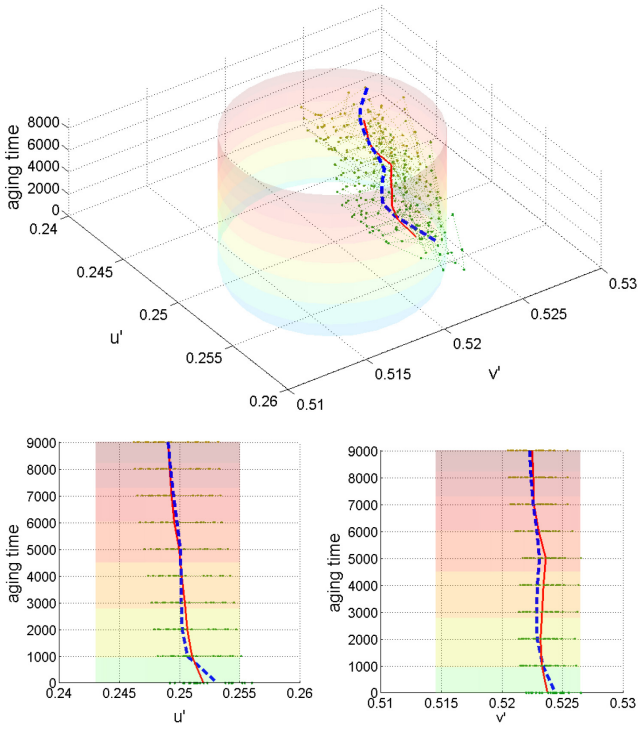

Figure 23 KF Chromaticity Tracking

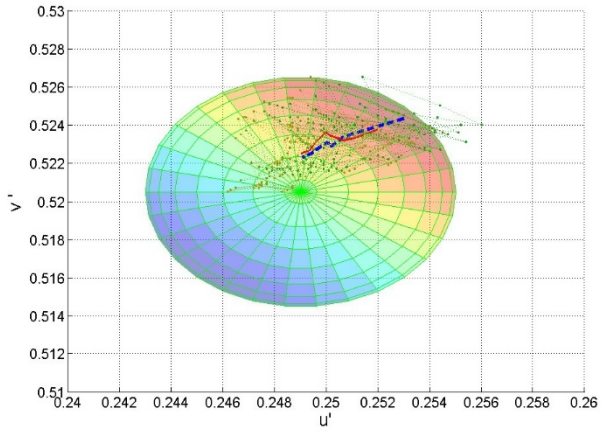

Figure 24 KF track with ± 0.06 confident interval

Shift of the (u', v') coordinates could indicate a major color shift which may render the LED unusable. The dash blue line is the KF chromaticity tracking for u' and v' in 9000 hours operating hours. Figure 24 shows u' v' KF tracking in 2D 1976 CIE u' v' coordinate. The circle is ± 0.06 confident interval; the circle center is central point for 3000K.

Life Distribution Fit

Cumulative distribution function F(t) represents the population fraction failing by age t. The reliability function R(t) for a life distribution is the probability of survival beyond age t, namely, the survivor or survivorship function can be represented as:

$$R(t) = 1 - F(t) \tag{63}$$

Normal distribution, Lognormal distribution and Weibull distribution have been fit to the distribution of predicted L70 lifetimes from EKF.

Normal Distribution

Previously, the normal distribution has been used to describe the life of incandescent lamp filaments in the field of lighting. The Normal Cumulative Distribution Function is represented by:

$$F(y) = \int_{-\infty}^{y} \sqrt{2\pi\sigma^2} \cdot e^{\left(\frac{1}{2}\left(\frac{x-\mu}{\sigma}\right)^2\right)} dx, -\infty < y < +\infty \tag{64}$$

Normal Probability Density. The probability density is:

$$f(y) = (2\pi\sigma^2)^{-1/2} \cdot e^{[-(y-u)^2/(2\sigma)]}, -\infty < y < +\infty \tag{65}$$

Normal Reliability Function. The population fraction surviving age t is:

$$R(t) = 1 - \Phi[(t - \mu)/\sigma] \tag{66}$$

The KF prognostic pseudo L70 life follows the normal distribution with expectation μ (26118) and variance σ(8687.7).

The EKF reliability function, R(t), can thereby be written by:

$$R(t) = 1 - F(t) = 1 - \Phi[(t - 43265)/ 2720.9] \tag{70}$$

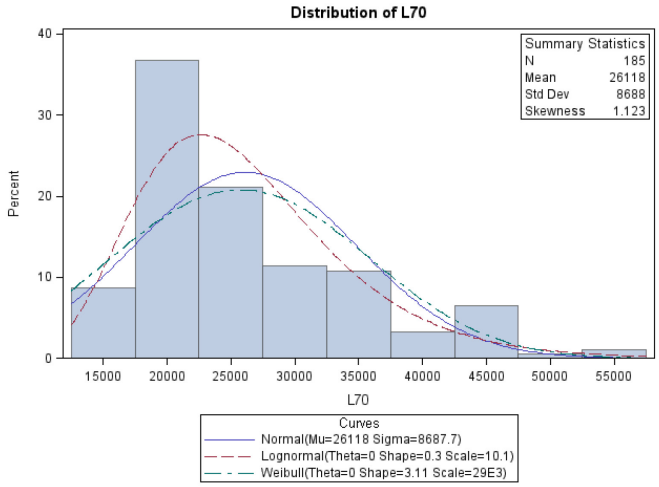

Figure 25 KF Distribution of L70

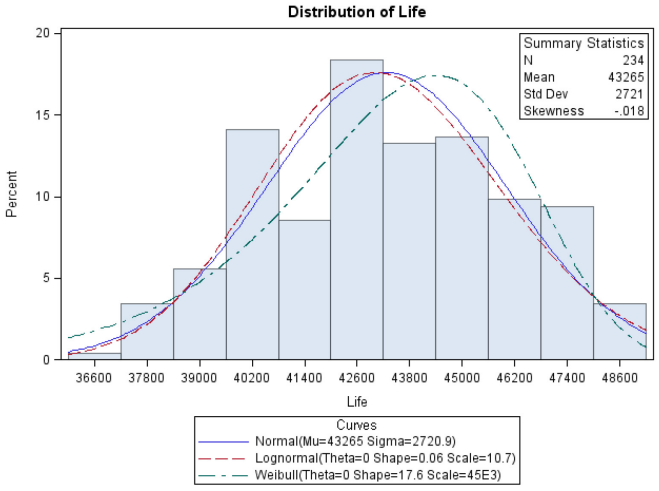

Figure 26 EKF Distribution of L70

Lognormal Distribution

The Lognormal distribution is widely used for life data or semiconductor failure mechanisms. The lognormal and normal distributions are related; this fact is used to analyze lognormal data with same methods for normal data.

Lognormal Cumulative Distribution is represented by:

$$F(t) = \Phi\{[\log(t) - \mu]/\sigma\}, t > 0 \tag{71}$$

Lognormal Probability Density function is represented by:

$$f(t) = \{0.4343/[(2\pi)^{1/2} t\sigma]\} \cdot e^{\{-[\log(t) - \mu]^2/(2\sigma^2)\}}, t > 0 \tag{72}$$

Lognormal Reliability Function is represented by:

$$R(t) = 1 - \Phi\{[\log(t) - \mu]/\sigma\} = \Phi\{-[\log(t) - \mu]/\sigma\} \tag{73}$$

The KF cumulative distribution of LEDs' L70 life would be written as the following function:

$$F(t) = \Phi[(t - 26118)/8687.7] \quad (67)$$

The KF reliability function, R(t), can thereby be written by:

$$R(t) = 1 - F(t) = 1 - \Phi[(t - 26118)/8687.7] \quad (68)$$

The EKF prognostic pseudo L70 life follows the normal distribution with expectation μ (43265) and variance σ(2720.9).

$$F(t) = \Phi[(t - 43265)/2720.9] \quad (69)$$

$$F(t) = \Phi\{[\log(t/10.122)]/0.3045\} \quad (74)$$

In the KF prognostic L70 distribution, we found that R(t) could be represented as:

$$R(t) = 1 - \Phi\{[\log(t/10.122)]/0.3045\} \quad (75)$$

$$= \Phi\{-[\log(t) - 24877]/0.3045\}$$

The EKF cumulative distribution of LEDs' L70 life would be written as the following function:

$$F(t) = \Phi\{[\log(t/10.7)]/0.06\} \quad (76)$$

In the LEDs' L70 distribution, we found that R(t) could be represented as:

$$\begin{aligned} R(t) &= 1 - \Phi\{[\log(t/10.7)]/0.06\} \\ &= \Phi\{-[\log(t) - 44356]/0.06\} \end{aligned} \quad (77)$$

Weibull Distribution

The Weibull distribution is often used for product life, because it models either increasing or decreasing failure rates simply. It is also used as the distribution for products properties such as strength (electrical or mechanical), elongation resistance (references), etc., in accelerated tests. It is used to describe the life of roller bearings, electronic components, ceramics, capacitors, and dielectrics in accelerated test. Weibull Cumulative Distribution. The population fraction failing by age t is:

$$F(t) = 1 - e^{-(t/\alpha)^{\beta}}, t > 0 \quad (78)$$

Weibull Probability Density is given by:

$$f(t) = (\beta/\alpha)t^{\beta-1} \cdot e^{-(t/\alpha)^{\beta}}, t > 0 \quad (79)$$

Weibull Reliability function is given by:

$$R(t) = e^{-(t/\alpha)^{\beta}}, t > 0 \quad (80)$$

The KF L70 life follows the Weibull distribution with the shape parameter β(3.11) and scale parameter α(29000).

$$F(t) = 1 - e^{[-(t/29000)^{3.11}]}, t > 0 \quad (81)$$

The reliability function, R(t), can thereby be written by:

$$R(t) = 1 - F(t) = e^{[-(t/29000)^{3.11}]}, t > 0 \quad (82)$$

The L70 life follows the Weibull distribution with the shape parameter β(17.6) and scale parameter α(45000).

$$F(t) = 1 - e^{[-(t/45000)^{17.6}]}, t > 0 \quad (83)$$

The reliability function, R(t), can thereby be written by:

$$R(t) = 1 - F(t) = e^{[-(t/45000)^{17.6}]}, t > 0 \quad (84)$$

Table 4 KF Distribution Fitted Statistic

Goodness-Fit Tests for Three Distributions		
Distributions	Cramer-von Mises Criterion	P-Value
Normal	1.161	<0.010
Lognormal	0.541	<0.005
Weibull	1.050	<0.010

Table 5 EKF Distribution Fitted Statistic

Goodness-Fit Tests for Three Distributions		
Distributions	Cramer-von Mises Criterion	P-Value
Normal	0.0968	<0.005

Table 4 and Table 5 respectively shows the fitting statistics for the Normal distribution, Lognormal distribution and Weibull distribution. The lower value of Cramer-von Mises Criterion (CMC-Minimum Distance), indicates a better fit of distribution. The lognormal distribution fitting shows lowest criterion value, indicating that it is the best fitting distribution.

The best fitted distribution for KF is lognormal distribution (Figure 25) with CMC value 0.541, and normal distribution (Figure 26) for EKF with CMC value 0.0968.

Summary and Conclusions

A life prediction methodology for L70 life of LEDs has been developed based on Kalman Filter and Extended Kalman Filter Models. Both the lumen degradation and the chromaticity shift have been predicted. The estimated state-space parameters based on lumen degradation and chromaticity were used to extrapolate the feature vector into the future and predict the time-to-failure at which the feature vector will cross the failure threshold of 70-percent lumen output. This procedure was repeated recursively until the LED failed. Remaining useful life was calculated based on the evolution of the state space feature vector. The KF/EKF estimations are range from 26,000 to 40,000 hours for the LEDs depending on the underlying degradation mechanism. Model predictions correlate reasonably with the TM-21 which provides L70 life-prediction in the neighborhood of 36,000 hours. Since the proposed computation method based on KF and EKF is recursive, any changes in underlying damage acceleration trigger updates to Kalman Gain and allow convergence of the model to measured lumen degradation. It has been shown that the KF and EKF based models can capture the underlying failure physics of multiple failure mechanisms active in the LEDs including (1) Silicone Encapsulate Degradation; (2) Chip Degradation; (3) Phosphor Degradation; (4) Reflector Degradation; and (5) Glass Degradation. Failure distributions of the L70 life have been constructed based on normal, lognormal and Weibull distributions. Normal distribution shows the best fit to the L70 histogram for the EKF model and the lognormal distribution shows the best fit for the L70 histogram for the KF model.

Acknowledgments

The work presented here in this paper has been supported by a research grant from the Department of Energy under Award Number DE-EE0005124.

References

Balchen, J. G, N. A Jenssen, E. Mathisen, and S. S\aelid. A Dynamic Positioning system based on Kalman Filtering and Optimal Control, Modeling, Identification and Control 1, No. 3, pp.135–163, 1980.

Banyasz, C., Csilla Bányász, László Keviczky, International Federation of Automatic Control, and International Federation of Operational Research Societies, Identification and system parameter estimation, Published for the International Federation of Automatic Control by Pergamon Press, 1992.

Baribeau, J., A lighting transformation, DOE Solid State Lighting R&D Workshop, Atlanta, GA, pp. 1-38, January 31–February 2, 2012

Bar-Shalom, Yaakov, X. Rong Li, Xiao-Rong Li, and Thiagalingam Kirubarajan, Estimation with Applications to Tracking and Navigation. John Wiley and Sons, 2001.

Batzel, T.D., and D.C. Swanson, Prognostic Health Management of Aircraft Power Generators, IEEE Transactions on Aerospace and Electronic Systems, Vol. 45, No. 2, pp. 473-482, 2009.

Bevly, D. M, and B. Parkinson. Cascaded Kalman filters for accurate estimation of multiple biases, dead-reckoning navigation, and full state feedback control of ground vehicles. IEEE Transactions on Control Systems Technology, Vol. 15, No. 2, pp. 199–208, 2007

CIE Publication 15:2, Colorimetry, Second edition: Vienna: Bureau Central CIE, 1986.

CIE Publication 15:2, Colorimetry, Third edition: Vienna: Bureau Central CIE, 2004.

Gueler, G. F. Modelling, Design and Analysis of an Autopilot for Submarine Vehicles, International Shipbuilding Progress 36, No. 405, pp. 51–85, 1989.

Hayward, R. C, D. Gebre-Egziabher, M. Schwall, J. D Powell, and J. Wilson. Inertially Aided GPS Based Attitude Heading Reference System (AHRS) for General Aviation Aircraft. In Proceedings of the Institute of Navigation ION-GPS Conference, pp. 1415–1424, 1997.

Herring, Kenneth D, and Frank Seiler, Evaluation of an Estimator for Real-Time Missile Tracking. Defense Technical Information Center, 1974.

IES TM-21, Projecting Long-Term Lumen Maintenance of LED Light Sources, pp. 1-28, 2011

Kalman, R., A New Approach to Linear Filtering and Prediction Problems, Transactions of the ASME--Journal of Basic Engineering, Vol. 82, No. D, pp. 35-45, 1960.

Kim, J. H, S. Wishart, and S. Sukkarieh. Real-time Navigation, Guidance and Control of a UAV using Low-cost Sensors, International Conference of Field and Service Robotics (FSR03), Japan, 2003.

Lall, P., Lowe, R., Goebel, K., Extended Kalman Filter Models and Resistance Spectroscopy for Prognostication and Health Monitoring of Leadfree Electronics Under Vibration, IEEE Transactions on Reliability, DOI: 10.1109/TR.2012.2220698, pp. 1-13, 2012.

Lall, P., Lowe, R., Goebel, K., Prognostics Health Management of Electronic Systems Under Mechanical Shock and Vibration Using Kalman Filter Models and Metrics, IEEE Transactions On Industrial Electronics, Vol. 59, No. 11, November 2012.

McCamy, C. S., Correlated color temperature as an explicit function of chromaticity coordinates, Color Research & Application 17 (2): 142–144. doi:10.1002/col.5080170211. plus erratum doi:10.1002/col.5080180222, 1992

Nelson, W., Accelerated Testing Statistical Models, Test Plans, and Data Analyses. Wiley-Interscience, 1st edition, 624 pages, September 21, 2004

Philips Lumileds: IESNA LM-80 Test Report, Design Resource DR05-1, Available at www.philipslumileds.com, March 7, 2012.

Poynton, C., Digital Video and HDTV, Morgan Kaufmann Publishers, 1st edition, 736 Pages, pp. 226, December 30, 2002.

Radkov, E., LED Lumen Maintenance Prediction Method, CORM Conference, Las Vegas, NV, pp. 1-28, May 2010

Saha, B. and K. Goebel, Modeling Li-ion Battery Capacity Depletion in a Particle Filtering Framework, Proceedings of the Annual Conference of the Prognostics and Health Mngt Society, http://www.phmsociety.org/node/167, San Diego, CA, pp. 1-10, 2009[a].

Saha, B., and K. Goebel, Uncertainty Management for Diagnostics and Prognostics of Batteries using Bayesian Techniques, Proceedings of the IEEE Aerospace Conference, Big Sky, MT, pp. 1-10, March 1-8, 2008.

Saha, B., Prognostics Methods for Battery Health Monitoring Using a Bayesian Framework, , IEEE Transactions on Instrumentation and Measurement, Vol. 58, No. 2, pp. 291-296, 2009[b].

Schanda, J., Colorimetry: Understanding the CIE System, Wiley-Interscience; 1st edition, 467 pages, pp. 81., August 10, 2007.

Solomou, S., Economic cycles. Manchester University Press ND, 1998.

Swanson, David, Michael Spencer, and Sevag Arzoumaniana, Prognostic Modeling of Crack Growth in a Tensioned Steel Band, Mechanical Systems and Signal Processing, Vol. 14, No. 5, pp. 789-803, September 2000.

Zarchan, P., and H. Musoff, Fundamentals of Kalman Filtering: A Practical Approach, Vol. 190. Progress in Astronautics and Aeronautics, American Institute of Aeronautics and Astronautics (AIAA), 2000.